

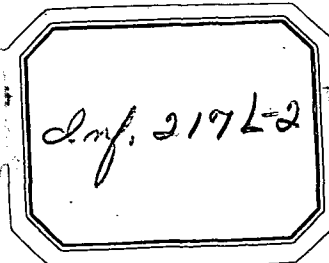
~~RESTRICTED~~

RM E52F23

NACA RM E52F23

CLASSIFICATION CHANGED

To Unclassified
 By authority of NACA Research
Directorate Date 1-18-53
12-11-53 mar



By 3

RESEARCH MEMORANDUM

(NACA-RM-E52F23) RADIANT HEAT TRANSFER
 FROM FLAMES IN A SINGLE TUBULAR TURBOJET
 COMBUSTOR (NASA) 31 p

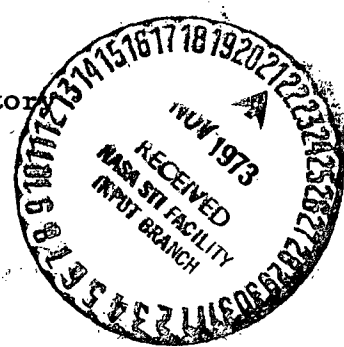
N73-74686

Unclas
 00/99 20995

RADIANT HEAT TRANSFER FROM FLAMES IN A SINGLE TUBULAR TURBOJET COMBUSTOR

By Leonard Topper

Lewis Flight Propulsion Laboratory
 Cleveland, Ohio



CLASSIFIED DOCUMENT

This material contains information affecting the National Defense of the United States within the meaning of the espionage laws, Title 18, U.S.C., Secs. 793 and 794, the transmission or revelation of which in any manner to an unauthorized person is prohibited by law.

CLASSIFICATION CHANGED

~~To Unclassified~~
 By authority of NACA Research
Directorate Date 1-18-53

12-11-53 mar

12-11-13

WASHINGTON
 August 19, 1952

~~RESTRICTED~~

~~RESTRICTED~~

NATIONAL ADVISORY COMMITTEE FOR AERONAUTICS

RESEARCH MEMORANDUMRADIANT HEAT TRANSFER FROM FLAMES IN A SINGLE TUBULAR
TURBOJET COMBUSTOR

By Leonard Topper

2634

SUMMARY

An investigation was conducted to determine the energy transfer by thermal radiation from the flame of a single tubular turbojet-engine combustor to the combustor liner. The effects of variations in combustor inlet-air pressure, fuel-air ratio, and air mass flow on the transfer of radiant energy were studied. The flame radiation parameters reported are equivalent black-body temperature, flame temperature, and flame emissivity. A total-radiation pyrometer was used to measure the black-body temperature of the flame; a modification of the two-color method was used to determine the average flame temperature.

The total radiation of the "luminous" flames (containing incandescent soot particles) was much greater (4 to 21 times) than the "nonluminous" molecular radiation due to carbon dioxide, water vapor, and other optically active molecules and radicals. The intensity of radiation from the flame increased rapidly with an increase in combustor inlet-air pressure; it was affected to a lesser degree by variations in fuel-air ratio and air mass flow. Measurable radiation energy was observed only in the primary zone; in this region the greater part of the total energy transfer may consist of radiation from the flame. Flame emissivities of 0.09 to 0.79 were observed.

INTRODUCTION

Quantitative information concerning the rate of energy transfer from flames of turbojet combustors is necessary for evaluating problems such as combustor-wall cooling, application of flame-heated fuel pre-vaporizers, and vaporization of fuel droplets from atomizers. The total energy transfer is composed of convection and radiation from the flame to the fuel spray and the combustor liner, and conduction through the liner. When wall cooling is used, the outside and usually also the inside of the liner are cooled in a convective process by a film of air flowing along the liner. During normal operation, the combustion gases are highly turbulent, and heat is transferred by the disorderly movement of eddies of gas. The rate of this convective process can usually

~~RESTRICTED~~

be expressed as a function of Reynolds number and Prandtl number, and it may be possible to estimate the convective transfer coefficient for heat flow from the flame to the wall from one of the familiar relations developed for fluids flowing in pipes (references 1 and 2).

Superposed on the convection process is that of thermal radiation. While the conduction and convection processes are affected only slightly by the temperature level, radiation increases quite rapidly with increase in temperature level. Thermal radiation may thus account for a large part of the total energy transfer, particularly in the primary zone, where gas temperatures are high, velocities are relatively low, and the flame emissivity is enhanced by the presence of incandescent soot particles (yellow "luminous" flame). 2634

Radiation from hydrocarbon flames can be of two distinct kinds: The nonluminous radiation consists of emission in certain regions of the infrared spectrum (due to simultaneous changes in the vibrational-rotational energy levels of heteropolar gas molecules) and also some visible and ultraviolet radiation. The luminous radiation is a continuous emission from flames made yellow by incandescent soot particles. Nonluminous radiation is always present and may be ascribed principally to carbon dioxide and water vapor. This type of radiation has been carefully studied at a total pressure of 1 atmosphere (reference 1), and there is some information on which to base extrapolation of the data to other total pressures (references 3 and 4). Such data may be used to predict the nonluminous radiation from flames. The prediction of the radiation to be expected from a luminous (yellow) flame is more difficult, since the soot concentration depends upon combustor design, degree of primary and secondary aeration, and combustor-inlet pressure. Useful information can be best obtained from experiments with combustors operated under actual conditions. The present investigation was undertaken at the NACA Lewis laboratory to determine the effect of operating conditions on flame radiation in a single turbojet combustor that is typical in design of a class of combustors, operated with MIL-F-5624 (grade JP-4) fuel.

The total radiation from a flame may be expressed by the equation

$$W = \epsilon \sigma T^4 \quad (1a)$$

or

$$W = \sigma T_B^4 \quad (1b)$$

where W is the total radiant energy emitted per unit area, σ is the Stefan-Boltzmann constant, and T is the absolute temperature. The emissivity ϵ is the ratio of the actual emissive power to that of a perfect radiator or black body. The use of the parameter equivalent

2634
black-body temperature of the flame T_B , as in equation (1b), is a convenient index for W . The total radiant energy W can be measured with a thermopile or a bolometer, and the flame temperature, by one of several different methods. Since the value of the Stefan-Boltzmann constant is accurately known, the emissivity can be calculated. In the study reported herein, the total radiation passing through a quartz window was measured with a total-radiation pyrometer having a blackened thermopile as the sensitive element. This pyrometer was calibrated against a black-body furnace to permit evaluation of equivalent black-body temperature of the flame. The red-brightness temperature of the flame was measured with an optical pyrometer. A new modification of the two-color pyrometer method (reference 5) was then used to compute the true flame temperature from the equivalent black-body temperature and the red-brightness temperature of the flame. A complete description of the method is presented in this report.

The preceding measurements were obtained at combustor inlet-air pressures from 13 to 96 inches of mercury absolute, air mass flows from 0.22 to 2.8 pounds per second, and fuel-air ratios from 0.008 to 0.035. The effects of these operating variables on black-body flame temperature and flame emissivity are presented. The investigation was conducted during March and April of 1952.

APPARATUS AND PROCEDURE

Combustor

A single tubular J33 combustor was modified by the addition of two pairs of sight holes ($1\frac{1}{4}$ inches in diameter) in the inner liner (figs. 1 and 2). The first pair of holes was 5 inches from the fuel nozzle. The tapered shell was equipped with cross tubes 3 inches long having an inside diameter of $1\frac{1}{4}$ inches, which were located in line with the inner sight holes. Quartz windows $1/4$ -inch thick were attached by flanges to the cross tubes.

The combustor was connected to the laboratory combustion air and exhaust service systems by ducting, as shown in figure 1. The air-flow rate and combustor pressure were manually regulated by remote-control butterfly valves.

Combustor Instrumentation

Air flow and fuel flow to the combustor were measured by means of an adjustable orifice and calibrated rotameters, respectively. The temperature of the inlet air was measured by a single-junction iron-constantan thermocouple located at instrumentation plane 3-3 (fig. 1).

The inlet-air pressure was measured by a static-pressure tap at plane 2-2. The combustor-outlet gas temperature was measured at plane 1-1 by 12 chromel-alumel thermocouples. The installation of these thermocouples is shown in figure 2. All temperatures were indicated on self-balancing potentiometers.

Flame Temperature and Radiation Measurement

The equivalent black-body temperature of the flame at each of the two observation stations was measured with a portable total-radiation pyrometer, which had been calibrated against a black-body furnace. The sensitive element of this instrument is a blackened thermopile on which the radiation is focused by a concave mirror. The thermopile responds nonselectively to radiation of all wavelengths. The red-brightness temperature was measured with a disappearing-filament optical pyrometer. An original method, based on the two-color principle (reference 5) was used to calculate average flame temperature and emissivity. A description of this method, together with sample calculations of flame temperature and emissivity, is presented in appendix A along with the details of the method used to correct the radiation measurements for the light transmission characteristics of the quartz window.

RESULTS

The flame-radiation data obtained over a range of combustor inlet-air pressure, air-flow rate, and fuel-air ratio at the first station (5 in. from the fuel nozzle) in the single combustor are presented in table I and in figures 3 and 4. Figure 3 compares the effect of combustor inlet-air pressure on equivalent black-body flame temperature at various air-flow rates and two fuel-air ratio ranges: 0.008 to 0.010 and 0.014 to 0.018 (fig. 3). These and other data are combined in figure 4 to compare this effect at various fuel-air ratios and three ranges of air-flow rate: 0.22 to 0.65, 1.4 to 1.8, and 2.8 pounds per second (figs. 4(a), 4(b), 4(c), respectively). Not all the data of table I have been presented graphically.

The greatest effect on black-body temperature of the flame was observed with variations in inlet-air pressure. Thus, at fuel-air ratios of 0.008 to 0.010 and an air flow of 2.8 pounds per second, an increase in pressure from 35 to 95 inches of mercury absolute was accompanied by an increase in black-body temperature from 1520° to 2490° R (fig. 3(a)), which is equivalent to a sevenfold increase in radiant energy. Similar increases were observed at the other fuel-air ratios and air-flow rates.

2634

The black-body temperature of the flame was influenced to a lesser degree by fuel-air ratio and by mass flow rate of air. At fuel-air ratios of 0.008 to 0.010, an increase in air flow from 1.4-1.5 to 2.8 pounds per second (fig. 3(a)) resulted in a slight increase in radiant intensity at pressures above 40 inches of mercury absolute. At fuel-air ratios of 0.014 to 0.018, however, the equivalent black-body temperature decreased very slightly with an increase in air flow from 0.45-0.65 to 1.8 pounds per second (fig. 3(b)); however, a further increase in air flow to 2.8 resulted in a marked decrease in black-body temperature. At mass flows of air from 0.22 to 1.8 pounds per second, the flame black-body temperature generally increased with an increase in fuel-air ratio (fig. 4). At the highest air-flow rate (2.8 lb/sec) a reverse trend was observed; thus, an increase in fuel-air ratio from 0.008-0.010 to 0.017 resulted in a significant decrease in black-body temperature.

Calculated values of the average flame temperature in the primary zone (fig. 5) remained essentially independent of air flow and of pressure at pressures greater than 80 inches of mercury absolute but were more than 200° F higher at fuel-air ratios of 0.008 to 0.010 than at fuel-air ratios of 0.014 to 0.017. The calculated flame temperature decreased rapidly as pressure was reduced. Computed total emissivities of the flame are presented in figure 6. The effects of pressure, air flow, and fuel-air ratio are similar to those observed for the black-body temperatures. The highest value of emissivity observed was 0.79 (at a pressure of 92 in. Hg abs., fuel-air ratio of 0.015, and air flow of 1.8 lb/sec), corresponding to an equivalent black-body temperature of 2790° R; the lowest value of emissivity observed was 0.09. Figures 5 and 6 present sufficient data to indicate the variation in flame temperature and emissivity. The complete set of data appears in table I.

The pressure at which the flame in the primary zone became blue depended on the fuel-air ratio and on the mass flow of air. At a fuel-air ratio of 0.035 and an air flow of 0.22 pounds per second, it was still yellow (red-brightness temperature, 2630° R) at a pressure of 15.5 inches of mercury absolute. At a fuel-air ratio of 0.016, a pressure of 20 inches of mercury absolute, and an air flow of 0.58 pounds per second, the flame luminosity was low (red-brightness temperature of 2480° R). At a fuel-air ratio of 0.009, a pressure of 45 inches of mercury absolute, and an air flow of 2.8 pounds per second, the red-brightness temperature observed was only 2460° R.

Only data for the upstream station are reported herein. The flame at the downstream station always had an equivalent black-body temperature too low for accurate measurement (below 1300° R) and was blue, so that the two-color method for computing true flame temperature was not applicable.

DISCUSSION

The variation in emissive power of the flame with pressure, fuel-air ratio, and air mass flow cannot be predicted on any purely theoretical grounds. It is reasonable, however, to assume that it will vary, at least qualitatively, in the same manner as does the local smoke density of the zone, the emissive power of which is under consideration. All the observed trends in radiant energy reported herein follow the trends in smoke density of turbojet-combustor exhaust gas reported in reference 6. For example, reference 6 shows that smoke density increases rapidly with pressure. Smoke density at lower fuel-air ratios (0.008 to 0.010) increases with air flow, but at fuel-air ratios above about 0.013 it decreases with increasing air flow. Increasing fuel-air ratio first increased and then decreased smoke density. Finally, the effect of changes in fuel-air ratio and air flow on smoke density was greater at the higher combustor inlet pressures.

Molecular radiation from carbon dioxide, water vapor, and other optically active molecules and radicals makes a much smaller contribution to the over-all transfer of energy than does radiation from luminous soot particles. In most cases, the observed total radiant energy was 4 to 21 times that estimated for a mixture of carbon dioxide and water vapor at the flame temperature and at partial pressures corresponding to complete conversion of the air in the primary combustion zone (table I). The actual ratio would be even higher since it is probable that some of the oxygen passes through the primary zone without being utilized for burning.

The design of the apparatus was such that the field viewed by the total-radiation pyrometer was essentially a cylinder, having as faces the two quartz windows at each station. A point located on the inside of the inner liner of the combustor would "see" an additional volume of flame upstream and also downstream of the zone viewed by the pyrometer. The equivalent beam length L (reference 1) for the pyrometer was 0.9 inch; that for the point on the combustor liner was 3.6 inches. If the flame were isotropic and an average value of the constant K (appendix A) were used, it would be possible to predict how much higher the emissivity would have been if the window had been located on the inner liner instead of being about 3 inches away. The effect of beam length on emissivity is presented in the following table:

Emissivity ϵ at beam length of	
0.9 in.	3.6 in.
0.10	0.34
.20	.60
.30	.76
.40	.87
.50	.94
.60	.97

This increase in emissivity would be reflected in a higher equivalent black-body temperature. An increase in emissivity from 0.30 to 0.76 would thus increase the equivalent black-body temperature from 2000° to 2520° R. The actual effect of the change in viewing position would be smaller than is indicated in the preceding table since the downstream gases had very little luminosity. The application of emissivity data is discussed in appendix B. Calculations indicate that the rate of radiant heat transfer to the combustor liner in the primary zone may be as large as a convective transfer corresponding to a heat-transfer coefficient of 50 Btu per hour per square foot per $^{\circ}$ F.

SUMMARY OF RESULTS

The following results were obtained from an investigation of the effects of combustor operating variables on the thermal radiation from the flame of a turbojet combustor:

1. The intensity of radiation from the flame increased rapidly with an increase in combustor inlet pressure and was affected to a lesser degree by variations in fuel-air ratio and air mass flow.
2. The total radiation of the luminous flames (containing incandescent soot particles) was much greater (4 to 21 times) than the molecular nonluminous radiation due to carbon dioxide and water vapor.
3. Over the observed range of operating conditions, measurable radiant energy was observed only in the primary zone; in this region the greater part of the total energy transfer to the liner may consist of radiation from the flame.
4. Flame emissivities of 0.09 to 0.79 were observed.

Lewis Flight Propulsion Laboratory
National Advisory Committee for Aeronautics
Cleveland, Ohio

APPENDIX A

CALCULATION OF TOTAL RADIATION, FLAME TEMPERATURE, AND EMISSIVITY

Analysis

A detailed discussion of heat transfer by radiation appears in reference 1. Experimental data for the emissivities of carbon dioxide and water vapor are presented as a function of temperature and the product $P_G L$, where P_G is the partial pressure of the particular gas in atmospheres and L is the equivalent beam length in feet for radiation. At temperatures above 2500° R, the gas emissivity decreases with increase in temperature and increases with increase in the term $P_G L$. All these data were obtained at total pressures of 1 atmosphere. Data at other pressures are limited but indicate that pressure broadening of the spectral lines makes Beer's law inapplicable (references 3 and 4) and that the value of the parameter $P_G L$ should be multiplied by $P_1/4$ before the charts for gas emissivity appearing in reference 1 are used.

The exact prediction of the emissivity of luminous flames on a theoretical basis is virtually impossible, but experimental evaluation has been simplified by the investigations of Hottel and Broughton (reference 5). Studies of the variation of the monochromatic absorptivity of luminous flames with wavelength showed that the absorptivity and emissivity decrease with increase in wavelength (fig. 7), and that the total emissivity is lower than the emissivity in the visible spectrum. A relation between monochromatic brightness temperature and the true flame temperature and emissivity was developed (reference 5) and made possible the determination of true flame temperature and emissivity from measurements of the brightness at two wavelengths with a special optical pyrometer. In the present investigation, this method was modified so that only standard readily available equipment was required. A total-radiation pyrometer was used to determine equivalent black-body temperature, and a conventional optical pyrometer, to measure red-brightness temperature. A trial-and-error procedure based on Hottel and Broughton's charts (figs. 8 and 9) was used to compute flame temperature and emissivity. This procedure assumes that all the radiant energy is from glowing soot particles and that the energy-wavelength distribution corresponds to that determined in reference 5. Equivalent black-body temperatures were adjusted for the contribution due to nonluminous radiation before they were used for calculating average flame temperatures.

The quartz window through which the flame was viewed absorbed and reflected some of the incident radiation and thus introduced a small error in the readings of both pyrometers. The reading of the optical

pyrometer was adjusted by adding the temperature correction shown in the following table (reference 7) to the observed red-brightness temperatures:

Observed temperature (°R)	Correction (°R)
1900	9.7
2300	15
2650	18
3000	23
3400	29
3700	36

The observed equivalent black-body temperature was corrected on the basis of the actual transmission-wavelength characteristics of the quartz window (fig. 10), and the computed energy-wavelength characteristic of the flame (fig. 11) based on reference 5.

The total emissivity was computed as the fourth power of the ratio of corrected black-body temperature to average flame temperature. Since the flame is nonisotropic, this value is not of a fundamental nature.

The two-color method of flame pyrometry, as originally developed, is based on the simultaneous solution of the two equations:

$$\frac{1}{T_R} - \frac{1}{T} = \frac{\lambda_R}{c_2} \log \epsilon_R \quad (A1)$$

$$\frac{1}{T_G} - \frac{1}{T} = \frac{\lambda_G}{c_2} \log \epsilon_G \quad (A2)$$

where

c_2 dimensional constant, 2.58 (cm)(°R)

T true flame temperature

T_G green-brightness temperature (at wavelength λ_G)

T_R red-brightness temperature (at wavelength $\lambda_R = 0.665 \mu$)

ϵ_G spectral absorptivity (or emissivity) at wavelength λ_G

ϵ_R spectral absorptivity (or emissivity) at wavelength λ_R

~~RESTRICTED~~

It is possible to express ϵ_λ as

$$\epsilon_\lambda = 1 - e^{-K_\lambda L} \quad (A3)$$

where

$$K_\lambda = K/\lambda\alpha$$

and

K_L absorption strength

K, α constants

K_λ constant dependent only on wavelength

L equivalent beam length of flame

In reference 5, the transmissivity of various flames was studied and it was concluded that a value of 1.39 should be used for α between 0.3 and 0.8 micron, and 0.95 between 0.8 and 10 microns. Uyehara (reference 8) used values of 1.32 and 1.05 for α . The computed flame temperature is insensitive to small changes in α . Hottel (reference 5) showed that for moderately thick flames, a change in the value of α used for the shorter wavelengths from 1.7 to 1.39 resulted in a change in flame temperature of only 14° R.

Evaluation of Light Transmission of Quartz Window

The fraction of the incident light which will be transmitted by the quartz window is given as

$$Tr_{av} = \frac{\int_0^\infty J_\lambda Tr_\lambda d\lambda}{\int_0^\infty J_\lambda d\lambda} \quad (A4)$$

where

J_λ intensity of incident radiation at wavelength λ

Tr_λ light transmission of quartz window at wavelength λ

λ wavelength of radiation

~~RESTRICTED~~

A plot of Tr_{λ} against λ for the quartz plate used in this investigation is shown in figure 10. An infrared spectrophotometer was used to obtain these data. Figure 11 indicates the variation of the relative luminous intensity $J_{\lambda}/\epsilon_{2\mu}$ with wavelength λ for flames having a temperature of 3460°R and having emissivities of 0.1, 0.5, 0.7, and 1.0 at λ of 2 microns. If the spectral emissivity were independent of wavelength, these curves would coincide; since 2 microns is close to the effective wavelength, the areas subtended by a given curve over and under 2 microns are approximately equal. The variation of the spectral transmission of the quartz window for light from hydrocarbon flames is shown in figure 12 and was calculated by use of equation (A4) and figures 10 and 11. These computations were made for flame temperatures of 2960°R and 3460°R and are summarized in the following table:

Temperature ($^{\circ}\text{R}$)	Emissivity ^a	Transmission of window Tr_{av}	Effective wavelength of flame radiation ^b (μ)
2960	1.0	0.690	2.33
2960	.5	.785	2.09
2960	.1	.870	1.96
3460	1.0	.770	2.10
3460	.7	.870	1.86
3460	.5	.875	1.83
3460	.1	.920	1.58

^aAt wavelength of 2 microns.

^bWavelength above which half the radiant energy of the flame lies.

The "cut-off" of the quartz window at about 4.0 microns is not a serious difficulty since only a relatively small portion of the total radiation is of longer wavelength. Thus, more than 80 percent of the luminous radiation is generally transmitted (see preceding table). The nonluminous radiation due to carbon dioxide and water vapor is only a small fraction of the total radiation.

It can be shown that the trial-and-error procedure used herein converges to the same values that would be obtained if Hottel's method based on red- and green-brightness temperatures were employed.

~~RECORDED~~

Sample Calculation of Equivalent Black-Body Temperature,
True Temperature, and Emissivity of Flame

The procedure used for computing the radiation characteristics of the flame is illustrated in the following paragraphs. The experimental data are those for point 1 (table I).

Experimental data:

Combustor inlet pressure, in. Hg. abs	28.8
Red-brightness temperature, $^{\circ}$ R	2800
Black-body temperature, $^{\circ}$ R	1810

Calculations:

As a first estimate of T , use $T = T_R = 2800^{\circ}$ R. By equations (1), the first estimate of emissivity is $\left(\frac{T_B}{T}\right)^4 = \left(\frac{1810}{2800}\right)^4 = 0.175$.

For $\epsilon = 0.175$ and $T = T_R = 2800^{\circ}$ R, the first estimate of KL (fig. 8) is 0.42.

For $KL = 0.42$ and $T_R = 2800^{\circ}$ R, the first computed flame temperature (fig. 9) is 2920° R.

For $\epsilon_{2\mu} = 0.175$ and $T = 2920^{\circ}$ R, the first estimate of the light transmission of the quartz plate (fig. 12) is 86 percent.

The corrected black-body temperature is $\frac{1810}{(0.86)^{1/4}} = 1870^{\circ}$ R.

Corrected red-brightness temperature is 2820° R (reference 7).

The black-body temperature associated with the radiation from carbon dioxide and water vapor (reference 1) is 1020° R.

The black-body temperature for luminous radiation alone is
 $(1870^4 - 1020^4)^{1/4} = 1830^{\circ}$ R.

For $T_B = 1830^{\circ}$ R and $T = 2920^{\circ}$ R, the first estimate of the luminous emissivity is $\left(\frac{1830}{2920}\right)^4 = 0.154$.

For $\epsilon = 0.154$ and $T = 2920^{\circ}$ R, the second estimate of KL (fig. 8) is 0.33.

For $KL = 0.33$ and $T_R = 2820^{\circ} R$, the second computed flame temperature (fig. 9) is $2990^{\circ} R$.

The second estimate of luminous emissivity is $\left(\frac{1830}{2990}\right)^4 = 0.140$.

For $\epsilon = 0.140$ and $T = 2990^{\circ} R$, the third estimate of KL (fig. 8) is 0.30.

For $KL = 0.30$ and $T_R = 2820^{\circ} R$, the third computed flame temperature (fig. 9) is $3040^{\circ} R$.

The third estimate of luminous emissivity is $\left(\frac{1830}{3040}\right)^4 = 0.132$.

For $\epsilon = 0.132$ and $T = 3040^{\circ} R$, the fourth estimate of KL (fig. 8) is 0.28.

For $KL = 0.28$ and $T_R = 2820^{\circ} R$, the fourth computed flame temperature (fig. 9) is $3060^{\circ} R$.

Since the fourth estimate is very close to the third, $T = 3060^{\circ} R$ is used. Then the total emissivity is $\left(\frac{1870}{3060}\right)^4 = 0.141$.

The first estimate of quartz light transmission is now checked and found to be correct.

APPENDIX B

APPLICATION OF EMISSIVITY DATA

The use of emissivities in computing radiant heat transfer from gases is as follows: Consider a cylinder of flame 6 inches in diameter and of infinite length, and assume an average flame temperature of 3200° R and emissivity of 0.50. Suppose the cylinder of flame is to be enclosed in a metal shell with temperature of 1800° R and emissivity equal to 0.90. Then the net transfer of heat from the flame envelope per foot of length is

$$q = \sigma A \epsilon_f \epsilon_s (T_f^4 - T_s^4) \quad (B1)$$

where

A area of flame, sq ft

T_f flame temperature, $^{\circ}$ R

T_s shell temperature, $^{\circ}$ R

ϵ_f emissivity of flame

ϵ_s emissivity of shell

σ Stefan-Boltzmann constant, 0.173×10^{-8} Btu/(sq ft)(hr) $(^{\circ}$ R) 4

$$q = (0.173 \times 10^{-8})(\pi/2)(0.50)(0.90)(104 \times 10^{12} - 10.5 \times 10^{12})$$

$$q = 11.4 \times 10^4 \text{ Btu}/(\text{hr})(\text{ft})$$

To transfer this quantity of heat by convection would require a film coefficient of at least $52(\text{Btu}/(\text{hr})(\text{sq ft})(^{\circ}\text{F}))$. If the flame and shell diameters are increased to 8 inches, the emissivity of the flame will be approximately 0.68 (equation (A3)). Then

$$q = \left(\frac{0.68}{0.50} \right) \left(\frac{8}{6} \right) (11.4 \times 10^4) = 18.2 \times 10^4 \text{ Btu}/(\text{hr})(\text{ft})$$

Since the flame volume has increased as

$$\left(\frac{8}{6} \right)^2 = 1.78$$

the radiant heat loss per unit volume is 90 percent of the former value.

REFERENCES

1. McAdams, William H.: Heat Transmission. McGraw-Hill Book Co., Inc., 2d ed., 1942.
2. Humble, Leroy V., Lowdermilk, Warren H., and Desmon, Leland G.: Measurements of Average Heat-Transfer and Friction Coefficients for Subsonic Flow of Air in Smooth Tubes at High Surface and Fluid Temperatures. NACA Rep. 1020, 1951. (Supersedes NACA RM's E7L31, E8L03, E50E23, E50H23.)
3. Kaplan, Lewis D.: On the Pressure Dependence of Radiative Heat Transfer in the Atmosphere. Jour. Meteorology, vol. 9, no. 1, 1952, pp. 1-12.
4. Matossi, Frank, and Rauscher, Emma: The Pressure Dependence of the Total Absorption in Infrared Bands. Zeitschr. f Phys., vol. 125, nos. 7-10, 1949, pp. 418-422.
5. Hottel, H. C., and Broughton, F. P.: Determination of True Temperature and Total Radiation from Luminous Gas Flames. Ind. Eng. Chem., Anal. Ed., vol. 4, no. 1, 1932, pp. 166-175.
6. Butze, Helmut F.: Effect of Inlet-Air and Fuel Parameters on Smoking Characteristics of a Single Tubular Turbojet-Engine Combustor. NACA RM E52A18, 1952.
7. Foote, Paul D., Fairchild, C. O., and Harrison, T. R.: Pyrometric Practice. Nat. Bur. Standards, Tech. Paper No. 170, Feb. 16, 1921.
8. Uyehara, O. A., Meyers, P. S., Watson, K. M., and Wilson, L. A.: Flame-Temperature Measurements in Internal-Combustion Engines. Trans. Am. Soc. Mech. Engrs., vol. 68, no. 1, 1946, pp. 17-30.



TABLE I - PERFORMANCE AND FLAME-RADIATION DATA OF SINGLE TUBULAR COMBUSTOR

Combustor inlet pressure (in. Hg abs)	Air flow (lb/sec)	Fuel flow (lb/hr)	Fuel-air ratio	Mean combustor outlet temperature (°R)	Combustion efficiency (percent)	Red-brightness temperature (°R)		Black-body temperature (°R)		Equivalent black-body temperature of non-luminous gases (°R)	Average flame temperature (°R)	Total emissivity	Ratio of total radiation to nonluminous radiation	Comments
						Observed	Corrected	Observed	Corrected					
28.8	0.22	28.0	.0350	1585	48	2800	2820	1810	1870	1020	3060	0.090	6.5	
20.5	.22	28.0	.0350	1510	43	2630	2650	1610	1660	910	2800	.122	11.1	
15.5	.22	28.0	.0350	1360	37	2610	2630	1460	1500	865	2860	.076	9.0	
51.0	.46	25.0	.0151	1180	58	2880	2900	2040	2140	1000	2990	.260	21.0	
51.0	.46	30.0	.0182	1385	66	2910	2930	2160	2260	1160	2970	.320	14.4	
62.0	.44	29.0	.0180	1410	68	2860	2880	2160	2260	1210	2960	.330	12.2	
28.0	.45	21.0	.0130	860	33	2770	2790	1670	1730	1000	2980	.117	9.0	
21.0	.45	28.0	.0180	1085	43	2560	2580	1550	1600	950	2700	.125	8.1	
13.1	.45	30.0	.0180	1060	41	2110	2120	1190	1220	800	2250	.085	---	Blue flame ^a
13.4	.45	36.0	.0220	1210	44	2140	2150	1290	1330	800	2280	.116	---	Blue flame ^a
16.0	.58	33.0	.0160	1060	47	2160	2170	1290	1340	800	2290	.117	---	Blue flame ^a
20.0	.58	33.0	.0160	1085	49	2460	2480	1480	1520	850	2550	.126	10.2	
26.0	.65	36.5	.0156	1060	47	2430	2450	1510	1565	950	2530	.146	7.4	
28.5	.64	57.5	.0248	1610	65	2675	2695	1700	1760	1020	2840	.148	8.8	
26.5	1.25	54.0	.0120	1100	61	2150	2160	1410	1460	800	2250	.178	---	Blue flame ^a
26.5	1.25	59.0	.0130	1160	67	2205	2215	1460	1520	930	2300	.190	---	Blue flame ^a
46.0	1.51	45.0	.0083	935	67	2820	2840	1650	1720	1200	3140	.090	4.2	
51.0	1.51	41.0	.0075	935	68	2840	2860	1790	1855	1200	3070	.134	5.8	
61.0	1.43	42.0	.0082	960	73	3010	3030	1910	1985	1230	3180	.152	6.8	
72.0	1.43	42.0	.0082	985	74	3060	3080	2050	2130	1290	3250	.185	7.5	
92.0	1.43	41.0	.0080	1010	78	3060	3080	2260	2330	1370	3170	.290	8.0	
81.0	1.47	44.0	.0083	1035	78	3060	3080	2160	2250	1320	3190	.250	8.4	
37.0	.97	28.0	.0080	1070	88	2710	2730	1660	1720	1010	2930	.119	8.4	
73.0	2.81	94.0	.0094	1260	100	3080	3100	2040	2120	1290	3250	.181	7.3	
85.0	2.81	95.0	.0094	1260	97	3110	3130	2280	2370	1315	3220	.293	10.5	
85.0	2.81	80.0	.0080	1270	100	3110	3130	2320	2410	1315	3170	.335	11.6	
76.0	2.81	82.0	.0081	1120	94	3100	3120	2180	2230	1320	3270	.215	8.1	
77.0	2.81	80.0	.0080	1260	98	3050	3070	2210	2290	1270	3120	.286	10.6	
96.0	2.81	97.0	.0096	1220	95	3155	3175	2360	2440	1380	3270	.310	9.9	
95.0	2.81	99.0	.0098	1310	100	3180	3210	2490	2580	1380	3220	.410	12.3	
80.0	2.81	96.0	.0095	1235	100	3100	3120	2220	2300	1325	3250	.250	9.2	
63.0	1.81	92.0	.0140	1585	100	2880	2900	2170	2270	1222	2950	.345	12.0	
77.0	1.81	97.0	.0150	1620	100	2860	2880	2415	2550	1260	2895	.625	16.8	
92.0	1.81	97.0	.0150	1685	100	2930	2950	2600	2790	1310	2960	.790	21.2	
94.0	2.81	170.0	.0169	1760	100	2850	2870	2190	2300	1310	2890	.405	9.5	
22.0	1.81	97.0	.0150	1310	76	2010	2030	1360	1420	800	2035	.240	---	Blue flame ^a
32.0	1.81	97.0	.0150	1410	87	2500	2520	1530	1590	950	2540	.155	7.8	
36.0	1.81	97.0	.0150	1485	91	2600	2620	1670	1730	1020	2740	.190	7.7	
41.0	1.81	147.0	.0225	1910	90	2600	2620	1680	1730	1060	2740	.190	7.2	
50.0	1.81	97.0	.0150	1585	100	2640	2660	2040	2150	1100	2670	.420	14.5	
62.0	1.81	92.0	.0142	1610	90	2780	2800	2280	2400	1370	2810	.530	9.3	
33.0	2.81	92.0	.0091	1080	79	2160	2170	1410	1460	---	2180	.200	---	Blue flame ^a
45.0	2.81	92.0	.0091	1160	90	2420	2460	1700	1770	1050	2465	.265	7.6	
62.0	2.81	92.0	.0091	1240	100	2750	2770	2060	2160	1200	2830	.340	10.6	
42.0	2.81	170.0	.0169	1520	83	2180	2190	1530	1605	---	2200	.285	---	Unsteady flame ^a
52.0	2.81	170.0	.0169	1620	91	2420	2440	1675	1755	1070	2470	.260	7.4	
65.0	2.81	170.0	.0169	1710	97	2590	2610	1685	1795	1170	2650	.300	8.2	

^aTrue flame temperature, equivalent black-body temperature, and emissivity values are uncertain.

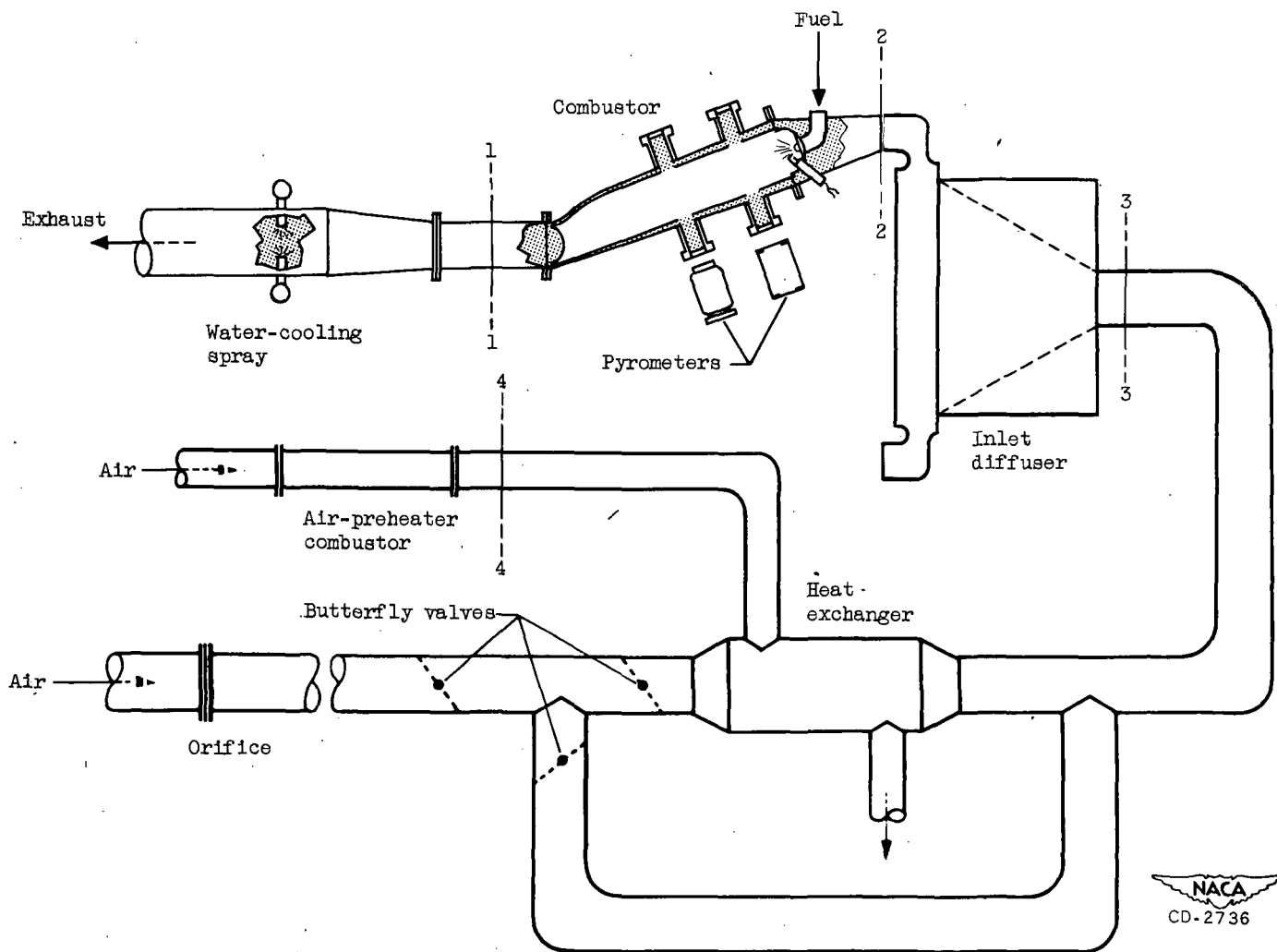
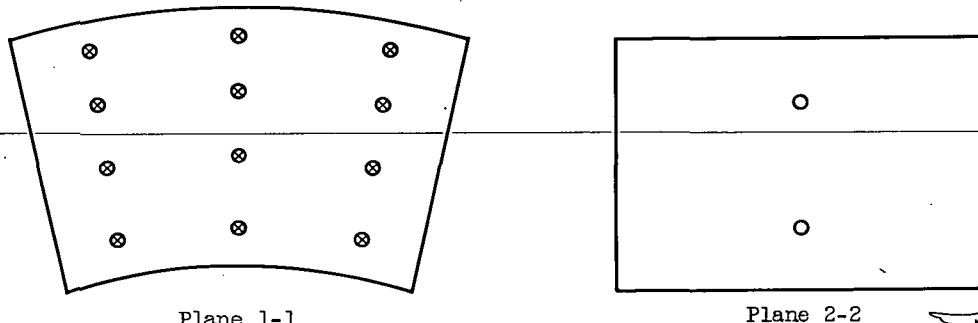
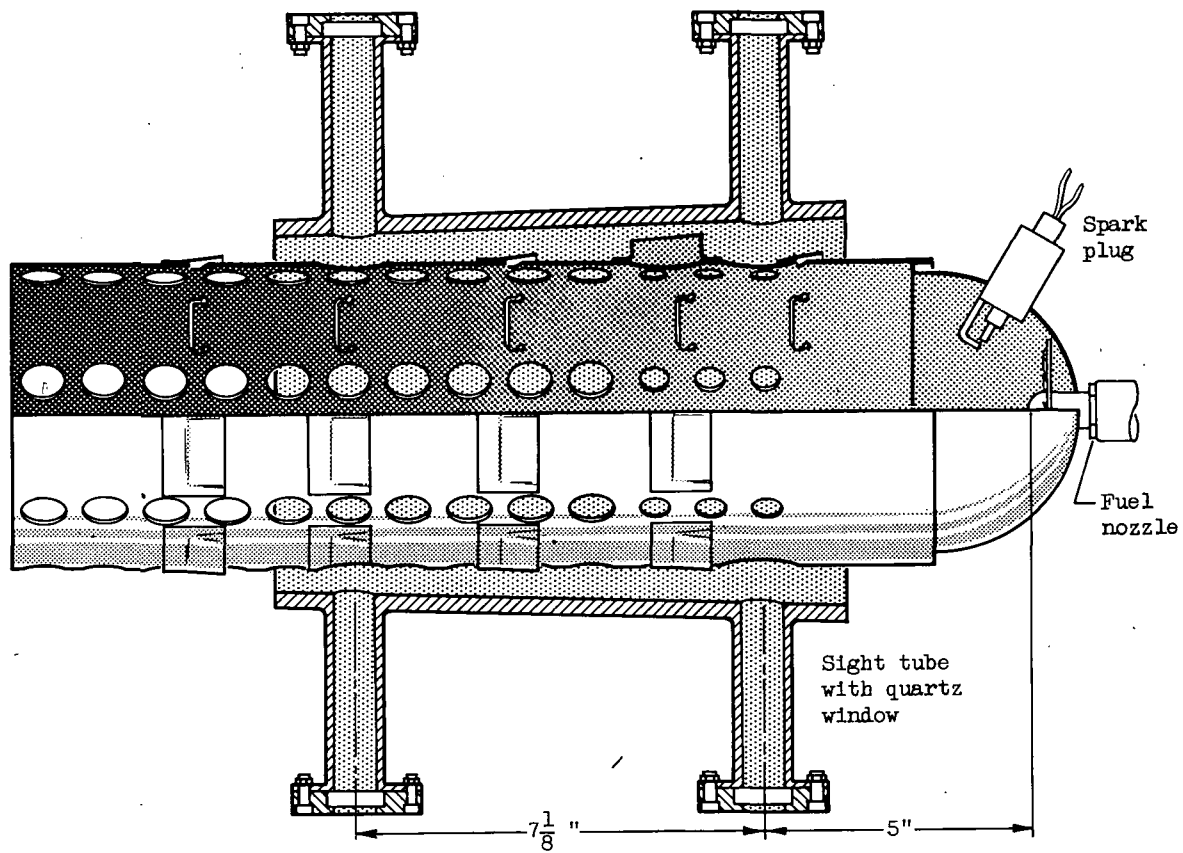


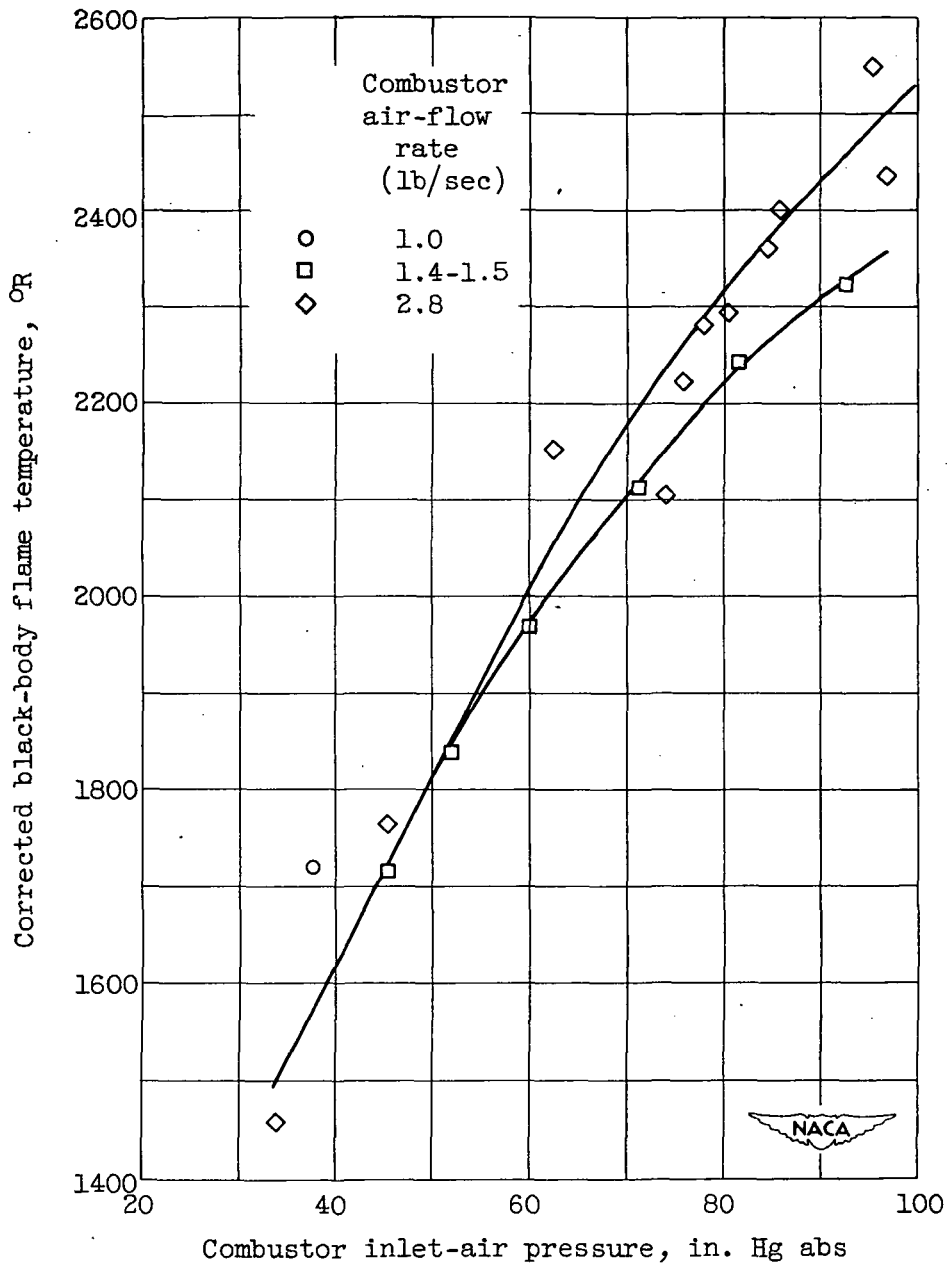
Figure 1. - Single-tubular-combustor installation, including location of instrumentation planes.



○ Static-pressure tap
⊗ Thermocouple

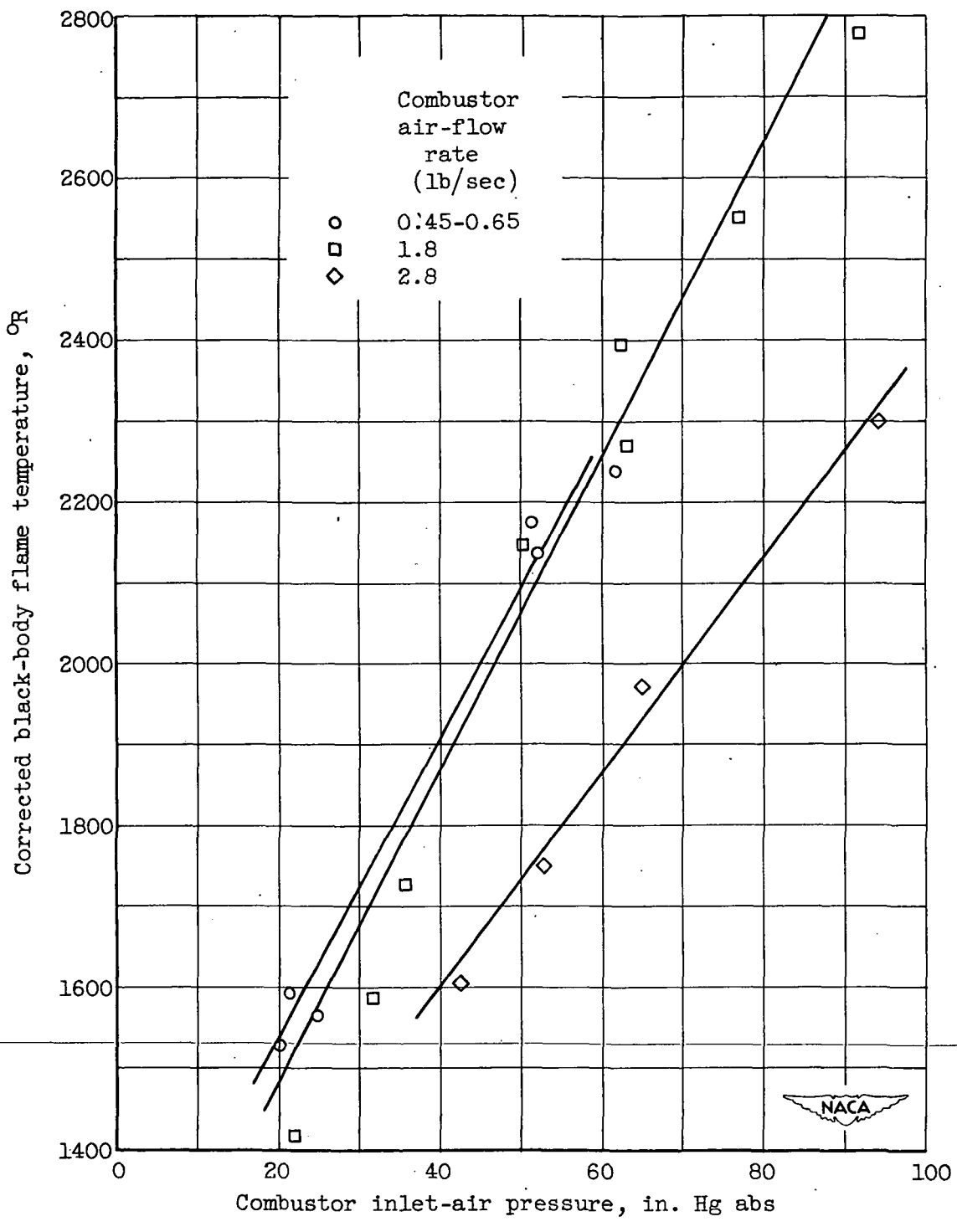
NACA
CD-2737

Figure 2. - Single tubular combustor modified for radiation studies, and arrangement of instrumentation planes of combustor installation.



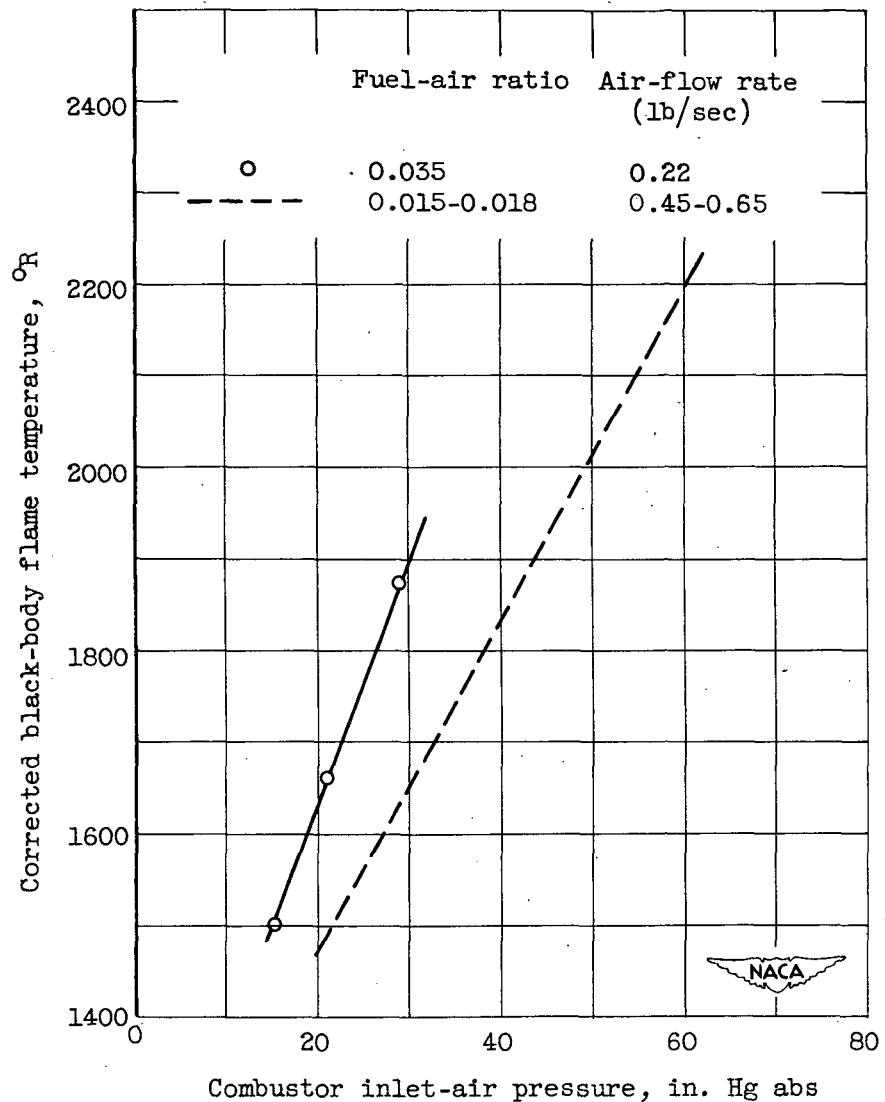
(a) Fuel-air ratio, 0.008-0.010.

Figure 3. - Effect of combustor inlet-air pressure on corrected black-body flame temperature at various combustor air-flow rates in single tubular combustor.



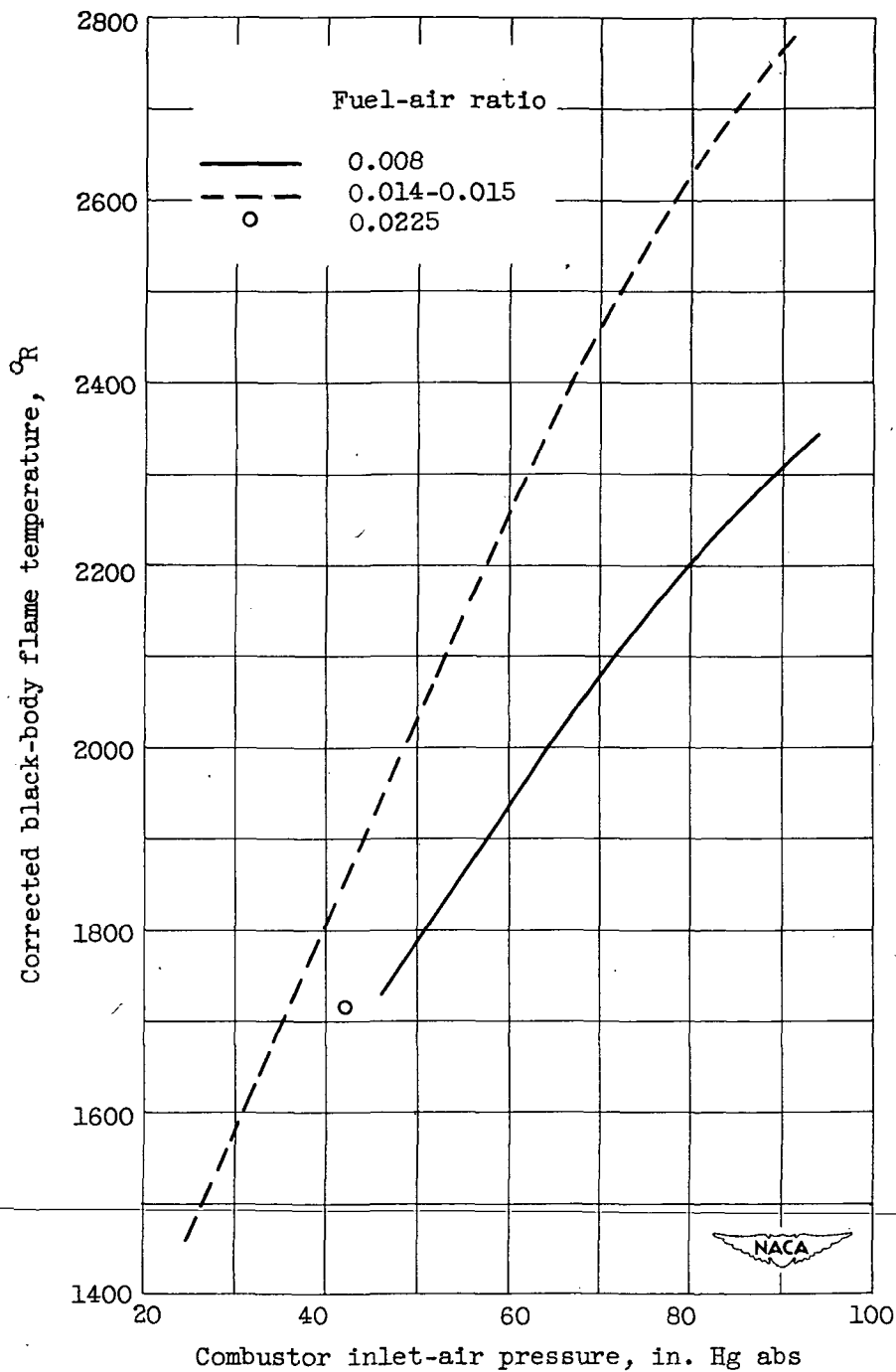
(b) Fuel-air ratio, 0.014-0.018.

Figure 3. - Concluded. Effect of combustor inlet-air pressure on corrected black-body flame temperature at various combustor air-flow rates in single tubular combustor.



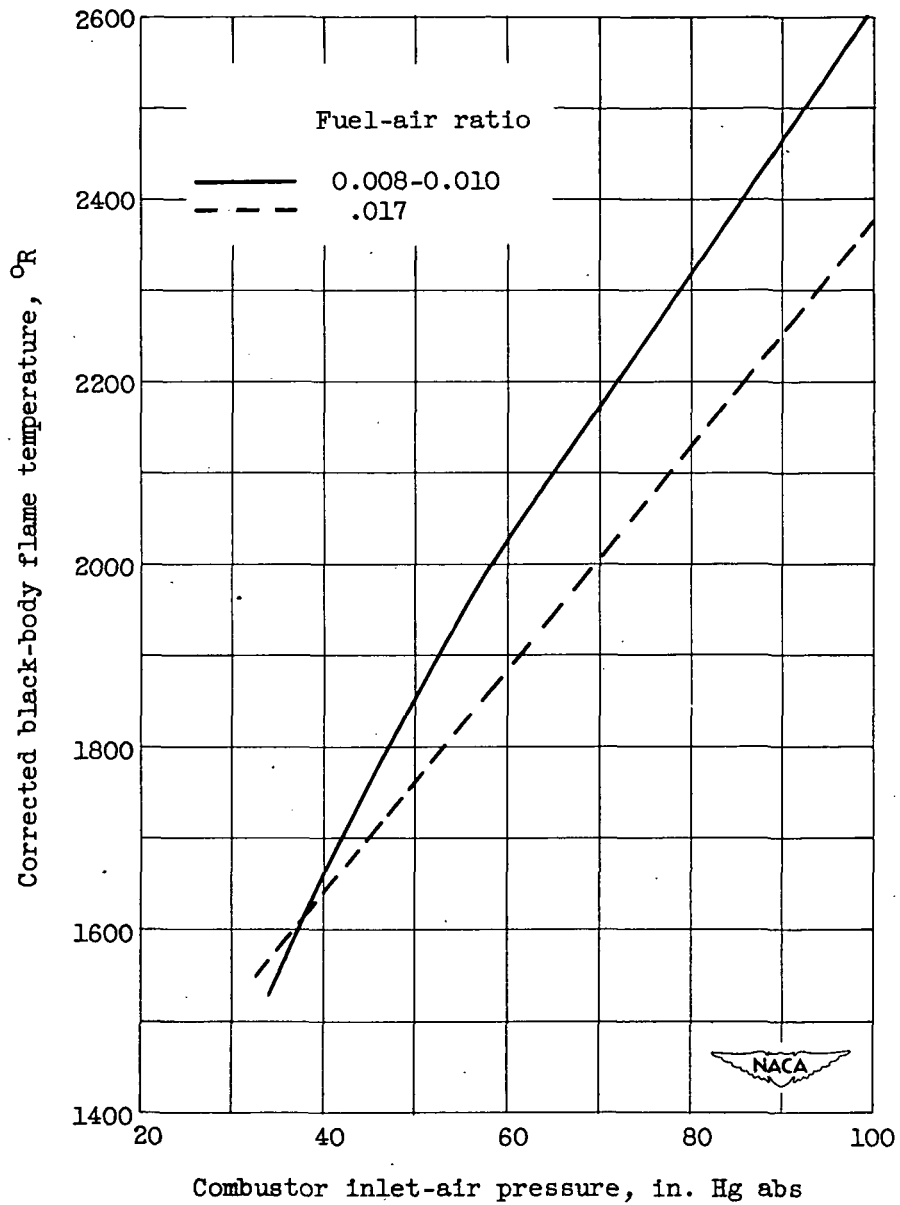
(a) Air mass flow, 0.22-0.65 pound per second.

Figure 4. - Effect of combustor inlet-air pressure on corrected black-body flame temperature at various combustor fuel-air ratios in single tubular combustor.



(b) Air mass flow, 1.4-1.8 pounds per second.

Figure 4. - Continued. Effect of combustor inlet-air pressure on corrected black-body flame temperature at various combustor fuel-air ratios in single tubular combustor.



(c) Air mass flow, 2.8 pounds per second.

Figure 4. - Concluded. Effect of combustor inlet-air pressure on corrected black-body flame temperature at various combustor fuel-air ratios in single tubular combustor.

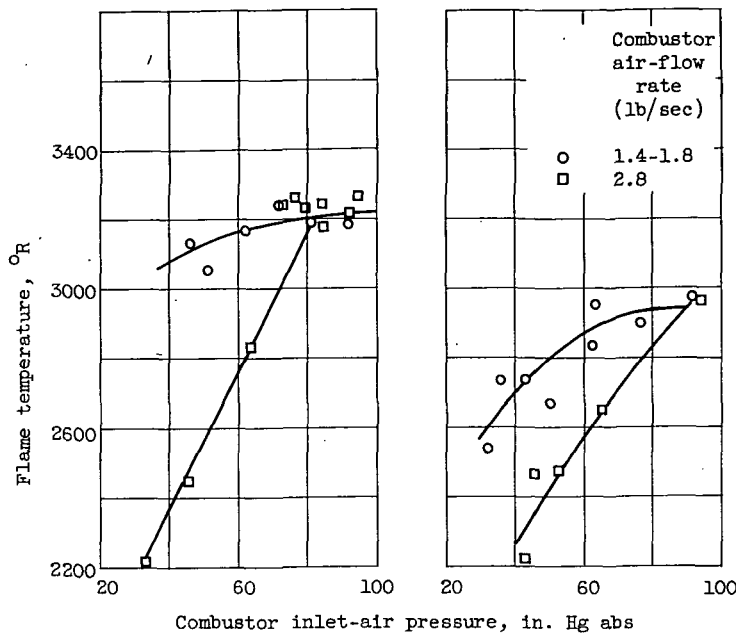


Figure 5. - Effect of combustor inlet-air pressure, fuel-air ratio, and air-flow rate on computed average flame temperature in single tubular combustor.

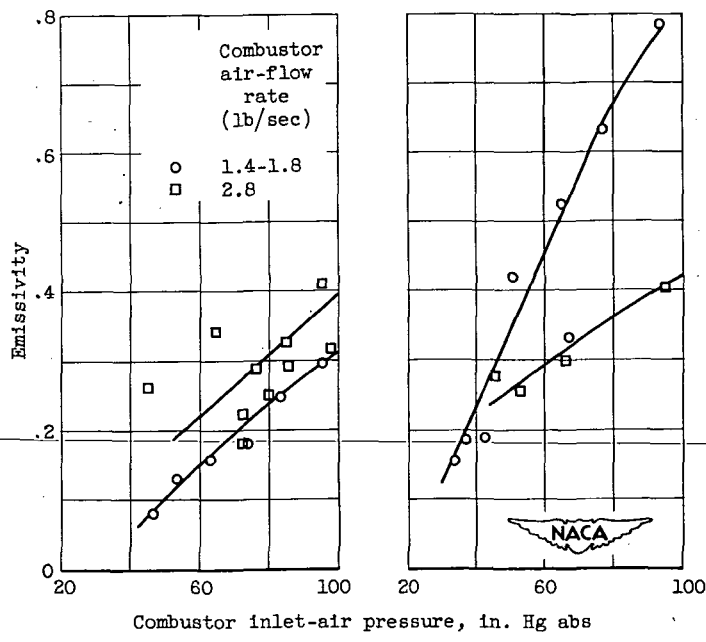


Figure 6. - Effect of combustor inlet-air pressure, fuel-air ratio, and air-flow rate on computed total emissivity of flames in single tubular combustor.

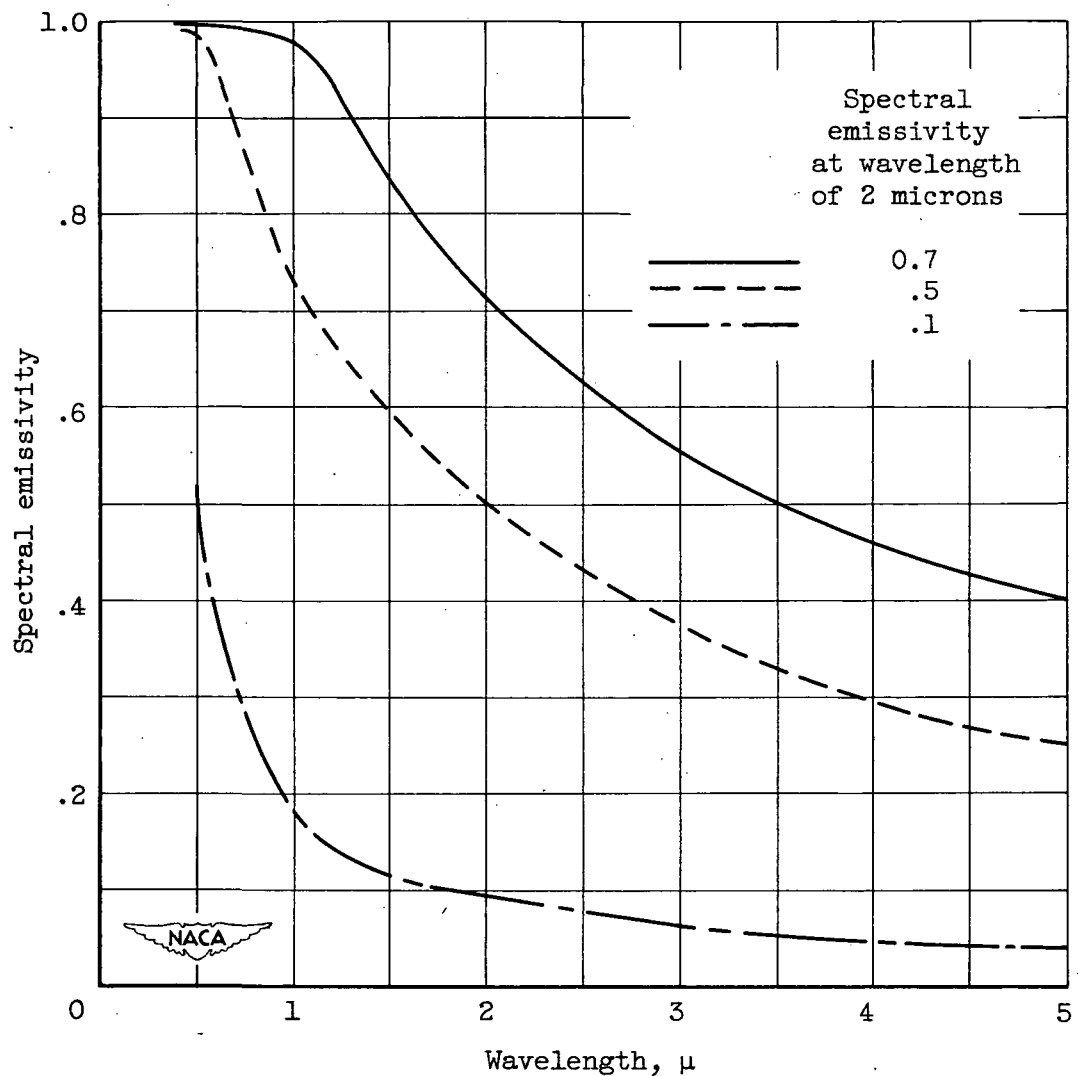


Figure 7. - Variation of spectral emissivity of hydrocarbon flames as function of wavelength for flames having certain spectral emissivities at wavelength of 2 microns.

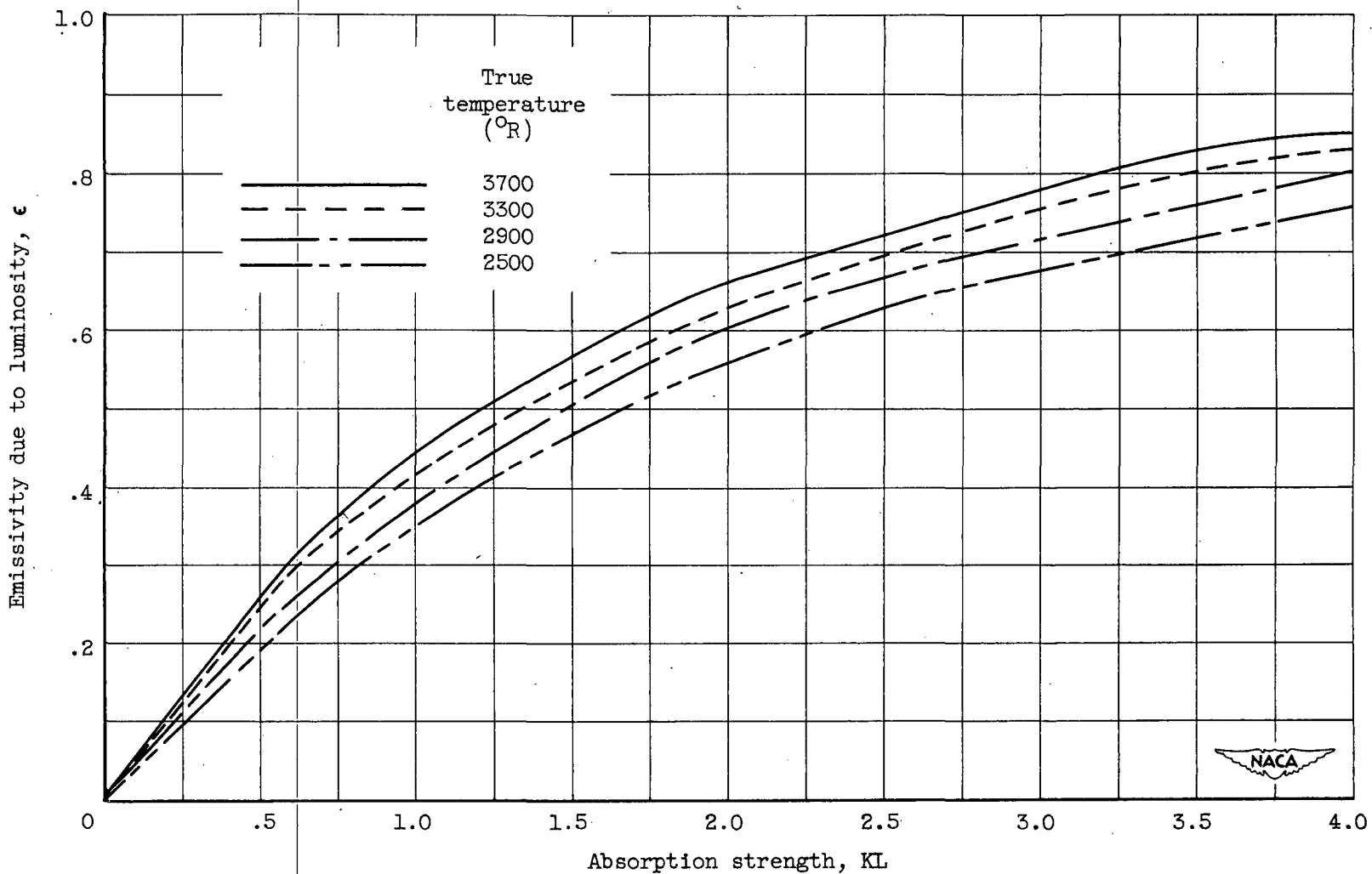


Figure 8. - Effect of absorption strength and temperature on luminous emissivity (reference 5).

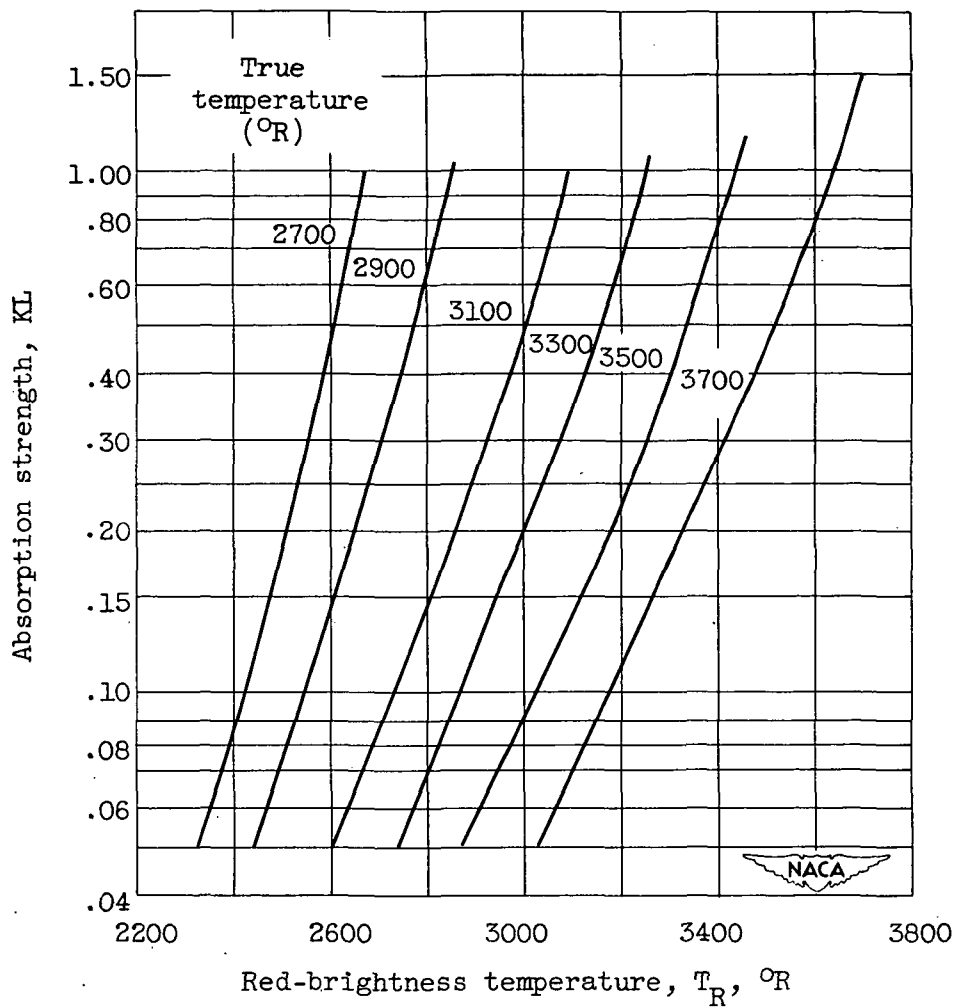


Figure 9. - Effect of true temperature and red-brightness temperature on absorption strength (reference 5).

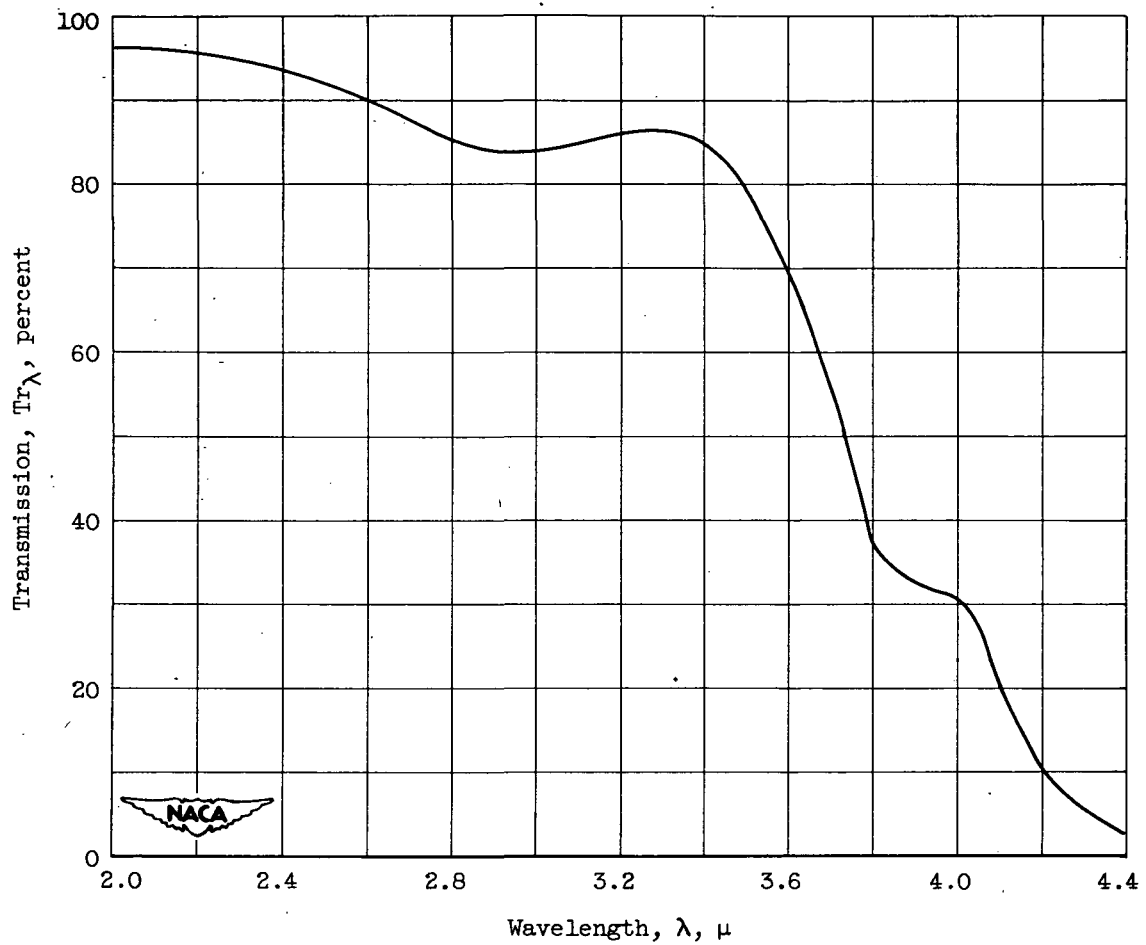


Figure 10. - Spectral transmission of quartz window used in flame-radiation study.

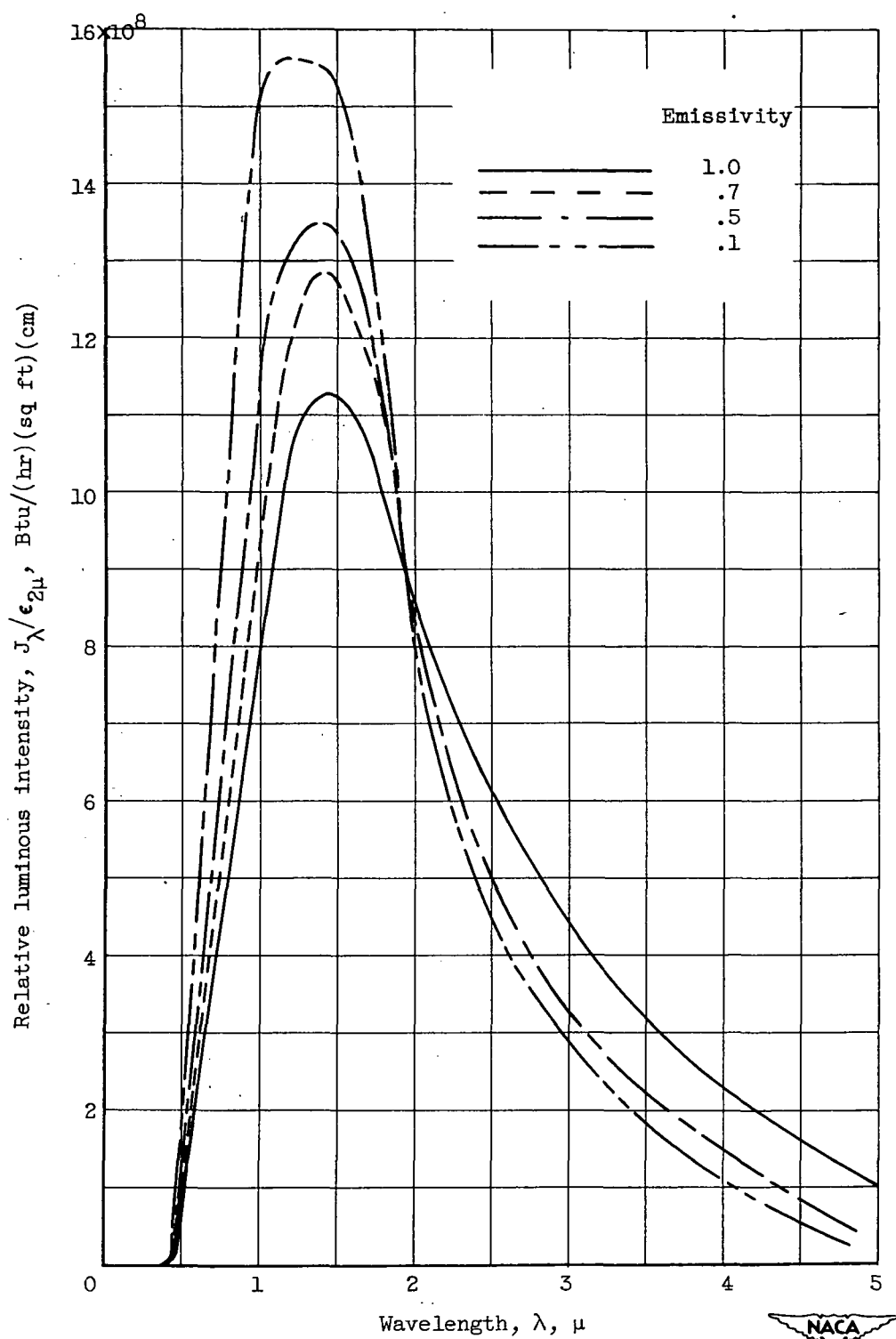


Figure 11. - Variation of relative luminous intensity of hydrocarbon flames with wavelength. Flame temperature, 3460° R.



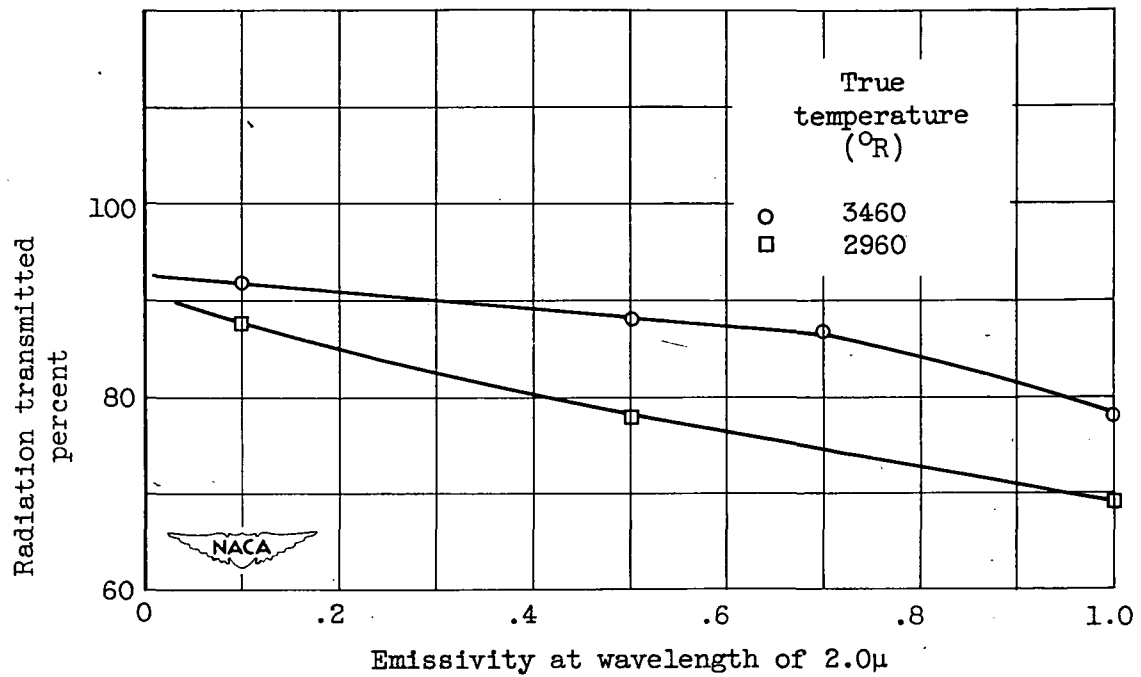


Figure 12. - Variation of average light transmission of quartz window used in flame-radiation study with temperature and emissivity of flame. Emissivity assumed equal to average emissivity.

~~SECURITY INFORMATION~~

~~RESTRICTED~~

CLASSIFICATION CHANGED

To Unclassified

By authority of

H36 Date 4/18/17

Med Research Abstract

~~RESTRICTED~~